ChemComm

Chemical Communications

Electronic Supplementary Information (19 pages)

Azulene Based Metal-Organic Frameworks for Strong Adsorption of H_2

Samir Barman[a], Hiroyasu Furukawa,*[b] Olivier Blacque,[a] Koushik Venkatesan, [a] Omar M. Yaghi[b] and Heinz Berke*[a]

[a] *Department of Inorganic Chemistry , University of Zürich Winterthurerstrasse 190, CH-8057, Zürich (Switzerland), E-mail: hberke@aci.uzh.ch, Fax: (+41) 44-635-6802*
[b] *Center for Reticular Chemistry, Department of Chemistry and Biochemistry, University of California-Los Angeles, 607 Charles E. Young Drive East, Los Angeles, California 90095. E-mail: furukawa@chem.ucla.edu*

Table of Contents

Section S1 *Materials and general procedures*

All solvents and reagents were purchased commercially and, unless otherwise noted, were used without further purification. Microanalyses were carried out at the Anorganisch-Chemisches Institut of the University of Zurich. IR spectra were obtained by using ATR methods with a Bio-Rad FTS-45 FTIR spectrometer. The powder XRD patterns were obtained with a Bruker D8 Advance system equipped with Cu sealed tube (λ = 1.5406 Å). The following conditions were applied: 40 kV, 40 mA, increment = 0.007°, scan speed = 1.5 s / step. The simulated powder patterns were calculated from the single crystal X-ray diffraction data and generated with Mercury 2.2 software. All TGA experiments were performed under a N_2 atmosphere from 25 - 800 °C at a temperature ramp rate of 5 °C / min.

Section S2 *Synthesis*

1,3-Azulenedicarboxylic acid, was prepared according to the published procedure.[S1]

Synthesis of $[Zn_5(\mu_3\text{-}OH)_2(\mathbf{L})_4(DMF)(H_2O)]\cdot(DMF)$ **(**MOF-645**).** [**L** = 1,3-azulenedicarboxylate]

A mixture of *N*,*N*-dimethylformamide (DMF)/ C_2H_5OH/ H_2O (1.00/0.25/0.25 mL) containing 1,3-azulenedicarboxylic acid (0.005 g, 2.3×10^{-5} mol) and $Zn(NO_3)_2\cdot 6H_2O$ (0.014 g, 4.62×10^{-5} mol) was sealed in a glass vial. The vial was heated (0.5 °C min^{-1}) to 90 °C for 48 h and then cooled at 0.1 °C min^{-1} to room temperature. The dark red crystals were washed with a DMF/ ethanol mixture (3 × 3 mL) to give (yield: 0.007 g, 88% based on 1,3-azulenedicarboxylic acid). Elemental analysis calcd (%) for $C_{54}H_{42}N_2O_{21}Zn_5$ = $[Zn_5(\mu_3\text{-}OH)_2(\mathbf{L})_4(DMF)(H_2O)]\cdot(DMF)$: C 46.94, H 3.06, N 2.03; found C 46.1, H 3.13, N 2.02.

Synthesis of $[Zn_4(\mu_4\text{-}O)(\mathbf{L})_3(DMF)_2]\cdot(DMF)_{1.25}(H_2O)$ **(**MOF-646**).**

1,3-azulenedicarboxylic acid (0.010 g, 4.6×10^{-5} mol) and $Zn(CH_3COO)_2\cdot 2H_2O$ (0.010 g, 4.62×10^{-5} mol) were combined with 2 mL of DMF and sealed in a glass vial and sonicated for several minutes. The vial was heated to (2.0 °C min^{-1}) 120 °C for 20 h in a controllable oven. The vial was taken out from the oven while hot and the hexagonal plate-shaped crystals were washed with DMF (3 × 2 mL) (Yield: 0.015 g, 80% based on the ligand). Elemental analysis calcd (%) for

$C_{45.75}H_{42.75}N_{3.25}O_{17.25}Zn_4$ = $[Zn_4(\mu_4\text{-}O)(\mathbf{L})_3(DMF)_2]\cdot(DMF)_{1.25}(H_2O)$: C 46.74, H 3.67, N 3.87; found C 46.54, H 3.61, N 4.26.

Activation of $[Zn_4(\mu_4\text{-}O)(\mathbf{L})_3(DMF)_2]\cdot(DMF)_{1.25}(H_2O)$ **(**MOF-646**).**

The activated form of MOF-646 was prepared either by heating MOF-646 under vacuum (< 10^{-3} torr) at 140 °C for 15 h or by evacuating at 45 °C following solvent exchange with chloroform. Elemental analysis calcd (%) for $C_{36}H_{18}O_{13}Zn_4$ = $[Zn_4O(\mathbf{L})_3]$: C 46.99, H 1.97, N 0.00; found C 46.35, H 1.98, N 0.00.

Section S3 *Crystallographic Data*

Single X-Ray Diffraction Studies on MOF-645 **and** MOF-646

Crystallographic data were collected at 153(2) K on an Oxford Xcalibur diffractometer (4-circle kappa platform, Ruby CCD detector and a single wavelength Enhance X-ray source with MoK_α radiation, λ = 0.71073 Å).[S2] The selected suitable single crystals were mounted using polybutene oil on the top of a glass fiber fixed on a goniometer head and immediately transferred to the diffractometer. Pre-experiment, data collection, analytical[S3] and multi-scan[S4] absorption corrections, and data reduction were performed with the Oxford program suite *CrysAlisPro*.[S4] The structures were solved with the Patterson (heavy atom) method and were refined by full-matrix least-squares methods on F^2 with SHELXL-97.[S5] All programs used during the crystal structure determination process are included in the WINGX software.[S6] The program PLATON[S7] was used to check the result of the X-ray analyses.

MOF-645 crystallizes in the non-centrosymmetric space group *C*2 with one solvent molecule of DMF per asymmetric unit. The solvent molecule is about a two-fold axis and positionally disordered over two positions with fixed site occupancy factors of 0.5:0.5. Soft restraints on its geometry and displacement parameters were used with the help of the DFIX, DELU and SIMU instructions of SHELXL-97.[S5] Three oxygen atoms (O2, O3 and O5) of carboxylate ligands are disordered over two positions with fixed site occupancy factors of 0.5:0.5. Constraints on their displacement parameters were applied using EADP. On the tetra-coordinate metal center Zn3, a substitutional disorder has been refined between coordinated DMF and water molecules with fixed site occupancy factors of 0.5:0.5. Only soft geometrical restraints (DFIX, DANG) were used to describe the positions of the hydrogen atoms of the water molecule. All other hydrogen positions were calculated after each cycle of refinement using a riding model, with C-H = 0.93 Å and $U_{iso}(H) = 1.2U_{eq}(C)$ for aromatic H atoms, with C-H = 0.98 Å and $U_{iso}(H) = 1.2U_{eq}(C)$ for the "methine" H atom on O1, and with C-H = 0.96 Å and $U_{iso}(H) = 1.5U_{eq}(C)$ for methyl H atoms.

MOF-646 crystallizes in the non-centrosymmetric space group $P2_1$ with two solvent molecules of DMF and eight molecules of water per asymmetric unit. In the crystal structure, the coordinated DMF molecule had to be partially refined over two positions with refined site occupancies of 0.435(14):0.565(14). Only soft restraints on displacement parameters (DELU,

SIMU) were used for selected carbon and oxygen atoms. All hydrogen positions were calculated after each cycle of refinement using a riding model, with C-H = 0.93 Å and $U_{iso}(H) = 1.2U_{eq}(C)$ for aromatic H atoms, and with C-H = 0.96 Å and $U_{iso}(H) = 1.5U_{eq}(C)$ for methyl H atoms.

Table S1. Summary of the X-ray diffraction studies of MOF-645 and MOF-646.

	MOF-645	MOF-646
empirical formula	$C_{51}H_{35}NO_{20}Zn_5$, C_3H_7NO	$(C_{84}H_{64}N_4O_{30}Zn_8)_2$, $5(C_3H_7NO)$, $4(H_2O)$
formula weight ($g \cdot mol^{-1}$)	1381.85	4702.25
temperature (K)	153(2)	153(2)
wavelength (Å)	0.71073	0.71073
crystal system, space group	monoclinic, *C* 2	monoclinic, *P* 2_1
a (Å)	15.7939(2)	17.2344(6)
b (Å)	16.6435(1)	17.2237(6)
c (Å)	12.2880(2)	17.2923(7)
α (°)	90	90
β (°)	123.831(2)	90.548(4)
γ (°)	90	90
volume ($Å^3$)	2683.19(9)	5132.8(3)
Z, density (calcd) ($Mg \cdot m^{-3}$)	2, 1.710	2, 1.521
abs coefficient (mm^{-1})	2.286	1.918
F(000)	1396	2392
crystal size (mm^3)	0.33 x 0.21 x 0.06	0.13 x 0.09 x 0.05
θ range (°)	2.6 to 32.6	2.4 to 25.7
reflections collected	39666	30148
reflections unique	9785 [R(int) = 0.0259]	17700 [R(int) = 0.0520]
completeness to θ (%)	99.9	99.9
absorption correction	semi-empirical from equivalents	analytical
max/min transmission	1.000 / 0.708	0.924 / 0.848
data / restraints / parameters	9785 / 76 / 416	17700 / 245 / 1302
goodness-of-fit on F^2	1.022	0.843
absolute structure parameter	0.007(7)	-0.003(11)
final R_1 and wR_2 indices [$I > 2\sigma(I)$]	0.0285, 0.0765	0.0468, 0.0931
R_1 and wR_2 indices (all data)	0.0307, 0.0770	0.0849, 0.0996

The unweighted R-factor is $R_1 = \sum(Fo - Fc)/\sum Fo$; $I > 2\sigma(I)$ *and the weighted R-factor is* $wR2 = \{\sum w(Fo^2 - Fc^2)^2/\sum w(Fo^2)^2\}^{1/2}$.

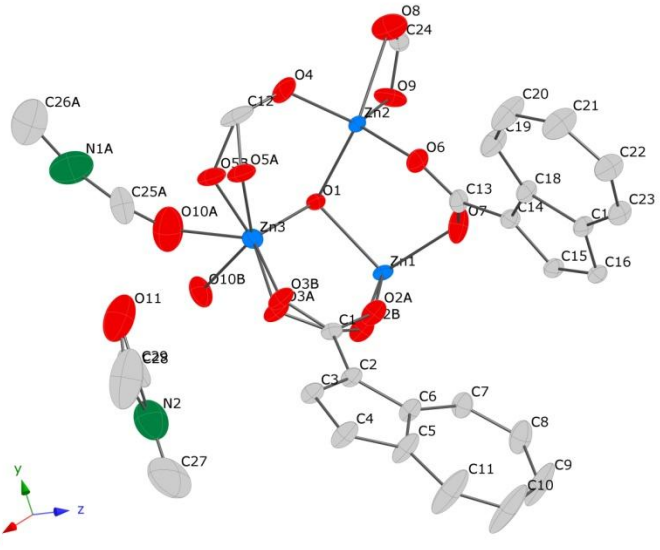

Fig. S1. ORTEP drawing (50% probability) of the asymmetric unit in MOF-645 is displayed with atomic labels. Three oxygen atoms (O2, O3 and O5) of carboxylate ligands are disordered over two positions with fixed site occupancy factors of 0.5:0.5. Color code: Zn, blue; N, dark green; O, red; C, gray. Hydrogen atoms have been omitted for simplicity.

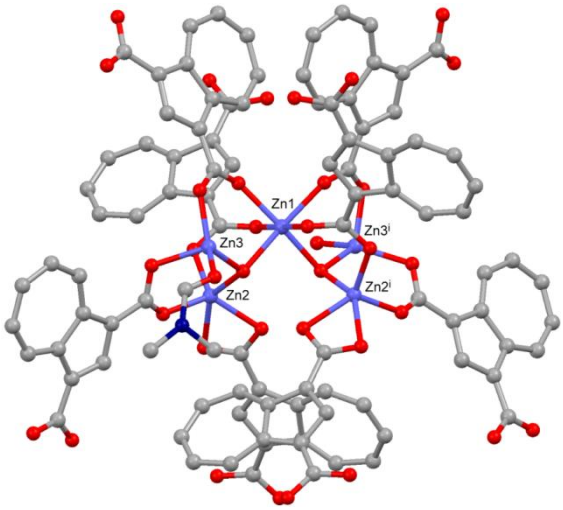

Fig. S2. A ball and stick presentation of the fundamental building unit of $[Zn_5(\mu_3\text{-}OH)_2(\mathbf{L})_4(DMF)(H_2O)]\cdot(DMF)$ (MOF-645). Color code: Zn, blue; N, dark blue; O, red; C, gray. Hydrogen atoms have been omitted for simplicity. Selected atom labels are shown.

a) b)

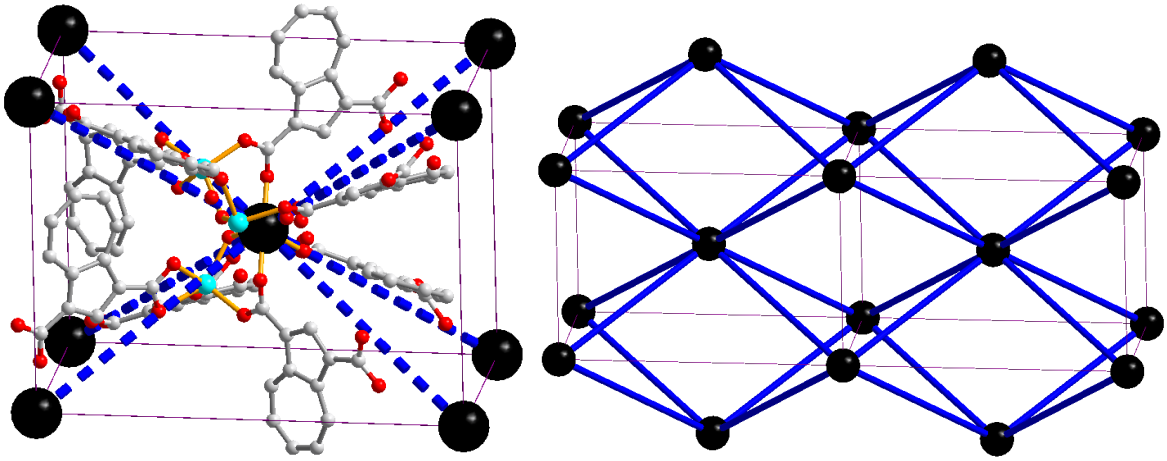

Fig. S3. X-ray structure of MOF-645: a) the topological view of MOF-645 in a cubic node; b) represents the fragment of the body-centered cubic lattice net (**bcu)** topology in MOF-645 stylized according to part a. (each of the vertices, black sphere, of a and b represents a $[Zn_5(\mu_3\text{-}OH)_2]$ clustering unit).

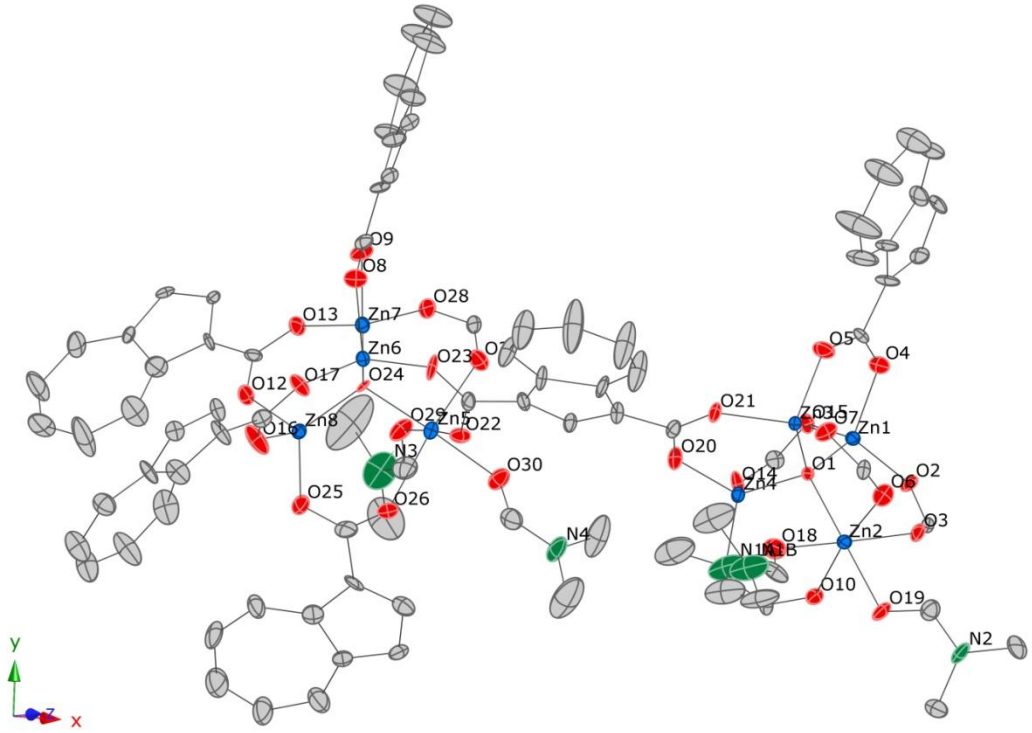

Fig. S4. ORTEP drawing (50% probability) of the asymmetric unit in MOF-646 is displayed with selected atomic labels. Color code: Zn, blue; N, dark green; O, red; C, gray. Hydrogen atoms have been omitted for simplicity.

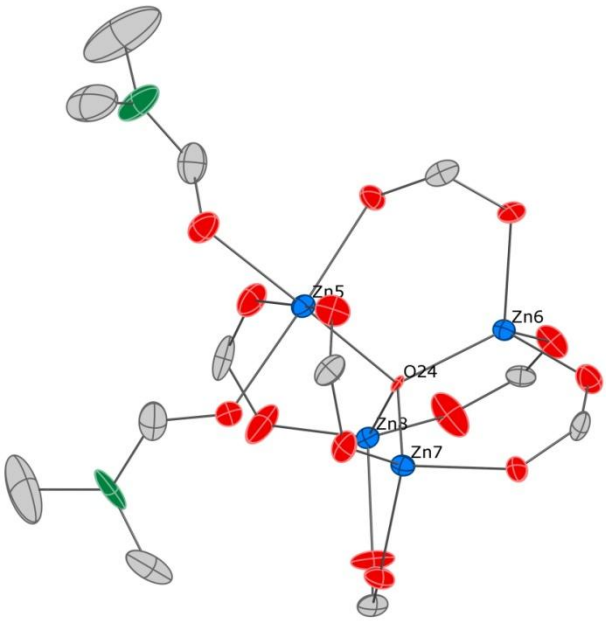

Fig. S5. ORTEP drawing (50% probability) of a $Zn_4(\mu_4\text{-O})$ unit in MOF-646 showing coordinated two DMF molecules.

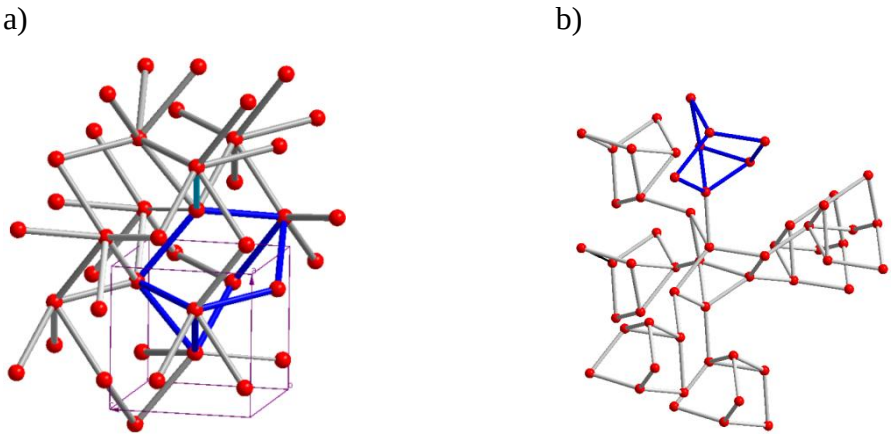

Fig. S6. a) and b) represent the fragment of the augmented **lcy** net and the extended 3D **lcy** net topology in MOF-646, respectively; the blue edges represent one kind of natural tiling [3.5^3] with one triangular and three pentagonal faces (each of the vertices, red sphere, represents the SBUs as shown in Fig. S5).

Section S4 *Powder X-Ray Diffraction Patterns*

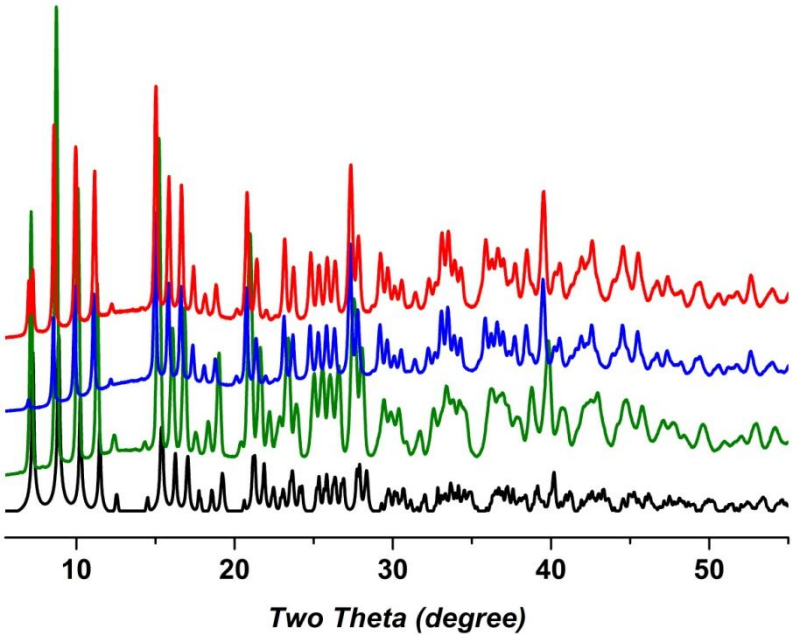

Fig. S7. Powder X-ray diffraction patterns: simulated from the single X-ray crystal structure of MOF-646 (black), as-prepared MOF-646 (olive), activated MOF-646 prepared by drying MOF-646 at 140 °C under vacuum for 15 h (blue) and sample prepared by evacuating at 45 °C for 36 h following solvent exchange with chloroform of MOF-646 (red).

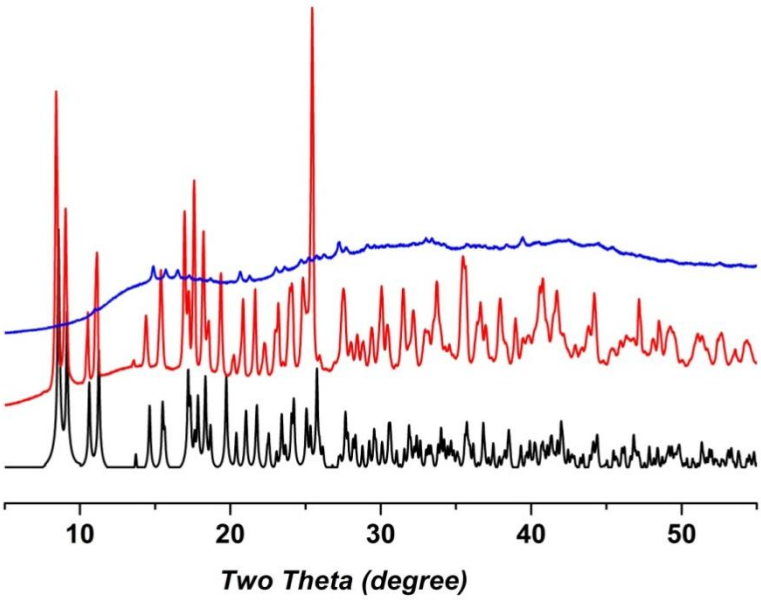

Fig. S8. Powder X-ray diffraction patterns for the simulation from the single crystal structure of MOF-645 (black), as-prepared MOF-645 (red) and MOF-645 drying at 200 °C for 18 h (blue).

Section S5 *IR Spectra*

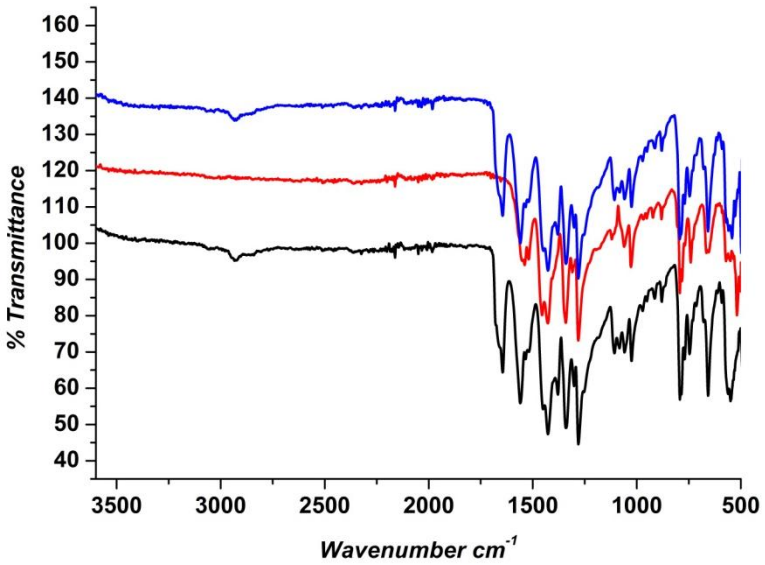

Fig. S9. ATR-IR spectra: as-synthesized MOF-646 (black), activated MOF-646 prepared by drying MOF-646 at 140 °C under vacuum for 15 h (red), sample obtained after immersing activated MOF-646 in DMF for 48 h at room temperature (blue)**.** Note that the C═O stretching frequency of DMF at 1645 cm^{-1} disappeared completely in activated MOF-646 and then reappeared upon soaking activated MOF-646 in DMF with almost the same intensity as was observed in the case of as-synthesized MOF-646.

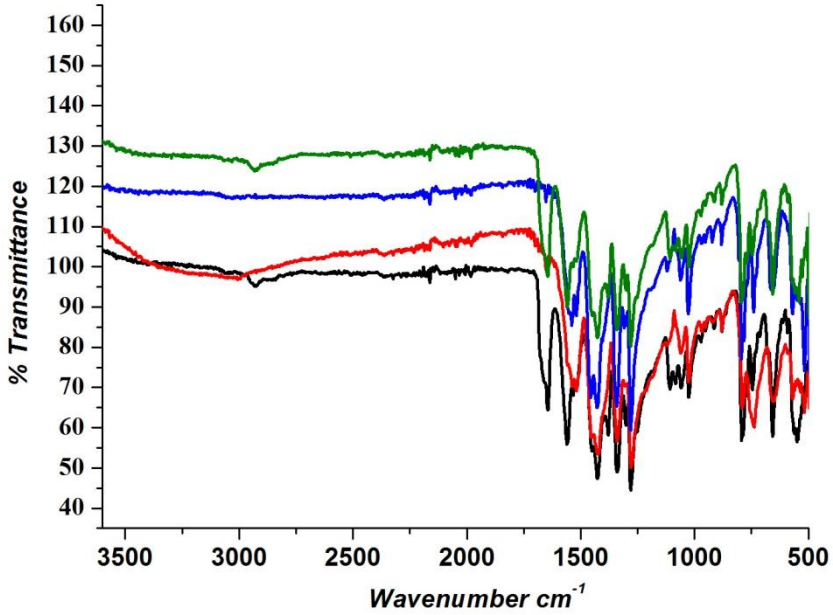

Fig. S10. ATR-IR spectra: as-synthesized MOF-646 (black), chloroform-exchanged sample of MOF-646 (red), sample prepared by evacuating at 45 °C for 36 h following solvent exchange with chloroform of MOF-646 (blue) and its re-solvated (immersion in DMF for 48 h at room temperature) form (olive).

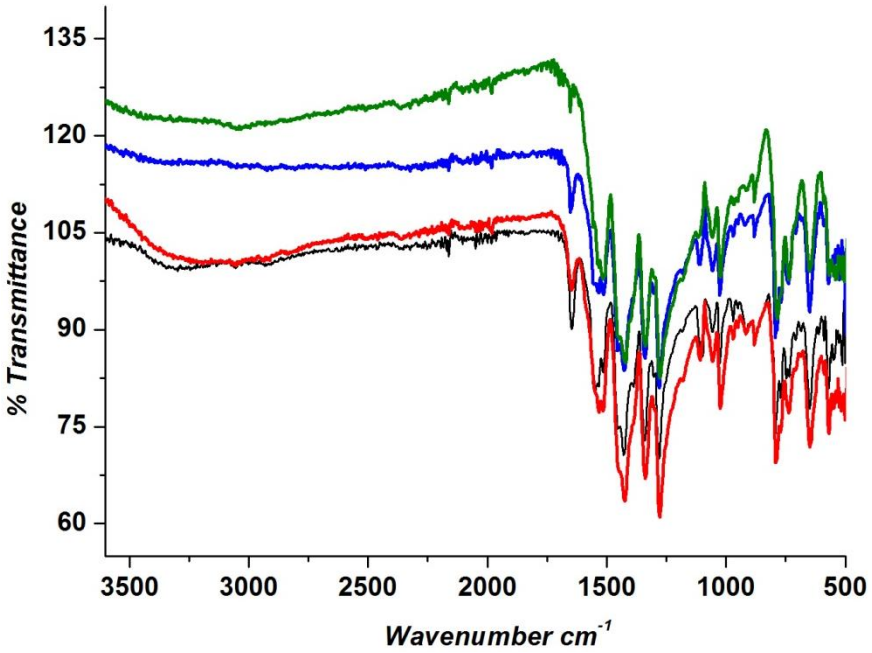

Fig. S11. ATR-IR spectra: as-synthesized MOF-645 (black), methanol-exchanged sample of MOF-645 (red), chloroform-exchanged sample of MOF-645 (blue), sample prepared by evacuating MOF-645 at 200 °C for 18 h (olive).

Section S6 *Thermal Gravimetric Analyses*

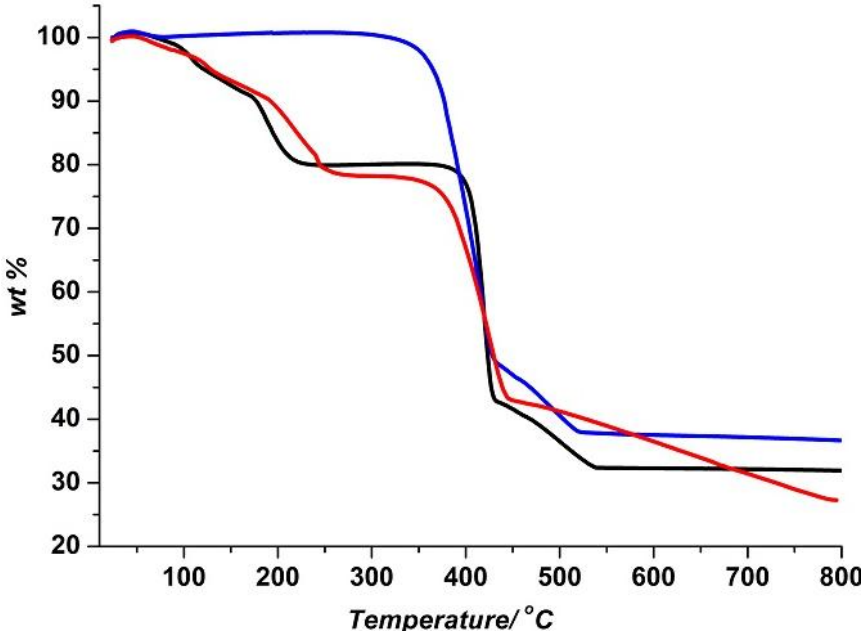

Fig. S12. TGA curves: as-synthesized MOF-646 (black), activated MOF-646 prepared by drying MOF-646 at 140 °C under vacuum for 15 h (blue) and sample obtained after immersing activated MOF-646 in DMF for 48 h at room temperature (red).

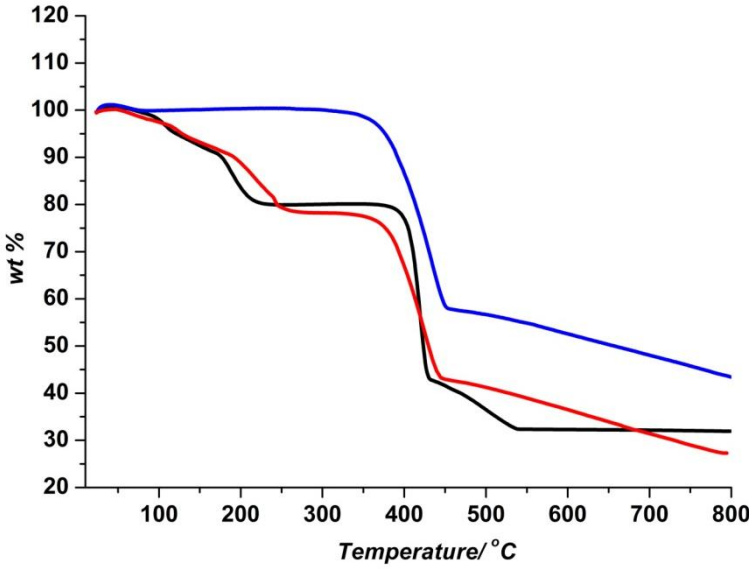

Fig. S13. TGA curves: as-synthesized MOF-646 (black), sample prepared by evacuating at 45 °C for 36 h following solvent exchange with chloroform of MOF-646 (blue) and its re-solvated (immersing in DMF for 48 h at room temperature) form (red).

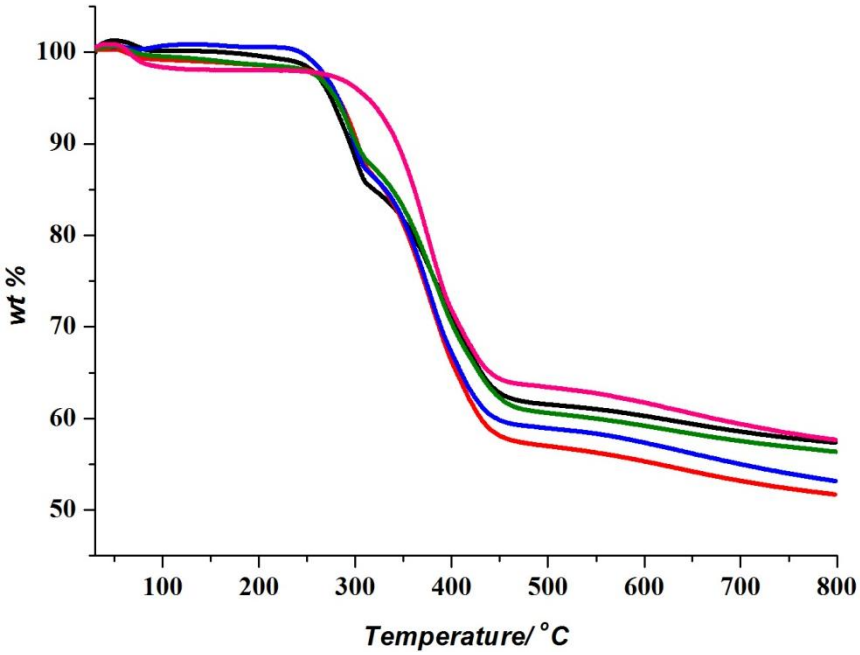

Fig. S14. TGA curves: as-synthesized MOF-645 (black), chloroform-exchanged sample of MOF-645 (red), methanol-exchanged sample of MOF-645 (blue), acetone-exchanged sample of MOF-645 (olive) and sample prepared by evacuating MOF-645 at 200 °C for 18 h (pink).

Section S7 *Gas Adsorption Measurements*

Low-pressure N_2, Ar, and H_2 adsorption measurements were performed on an Autosorb-1 (Quantachrome) volumetric analyzer.[S8] The samples were outgassed to 10^{-6} torr. Helium was used for the estimation of the dead volume, assuming that it is not adsorbed at any of the studied temperatures. Liquid N_2, and liquid Ar baths were used for adsorption measurements at 77 and 87 K, respectively. To provide high accuracy and precision in determining P/P_0, the saturation pressure P_0 was measured throughout the N_2 and Ar analyses by means of a dedicated saturation pressure transducer, which allowed us to monitor the vapor pressure for each data point. Ultra-high-purity grade Ar, N_2, H_2, and He (99.999% purity) were used throughout the adsorption experiments. Non-ideality of gases was obtained from the second virial coefficient at experimental temperature.[S9] Surface areas of the sample were determined from the N_2 as well as from the Ar adsorption isotherm for activated MOF-646, respectively. To estimate pore size distributions for activated MOF-646, Ar isotherms were analyzed using nonlocal density functional theory (NLDFT) implementing a hybrid kernel for Ar adsorption at 87 K based on a zeolite/silica model containing cylindrical pores.[S10] The cumulative pore volume for activated MOF-646 was calculated from a NLDFT fit to the Ar adsorption data for activated MOF-646.

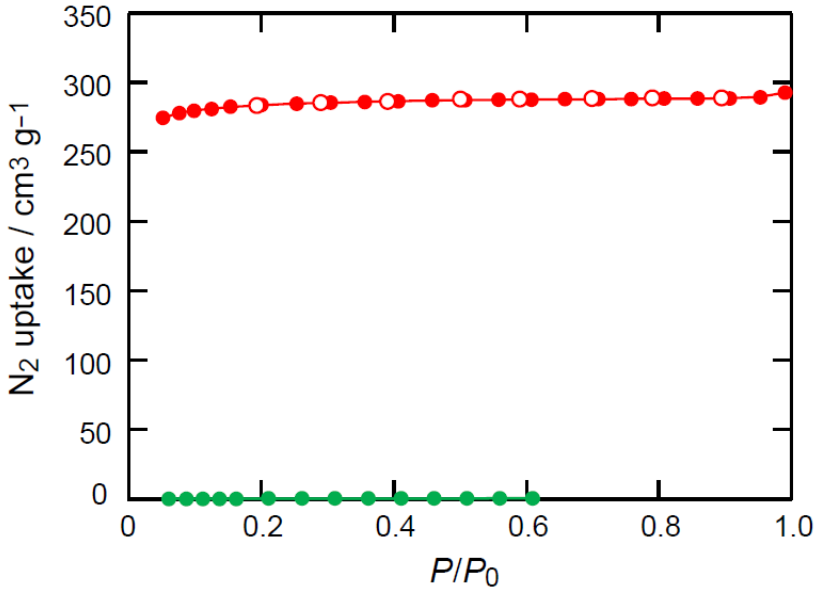

Fig. S15. N_2 isotherm at 77 K: activated MOF-646 (red), MOF-645 degassed at 200 °C for 14 h (olive). Filled and open circles represent adsorption and desorption branches, respectively. Connecting traces are guides for the eyes.

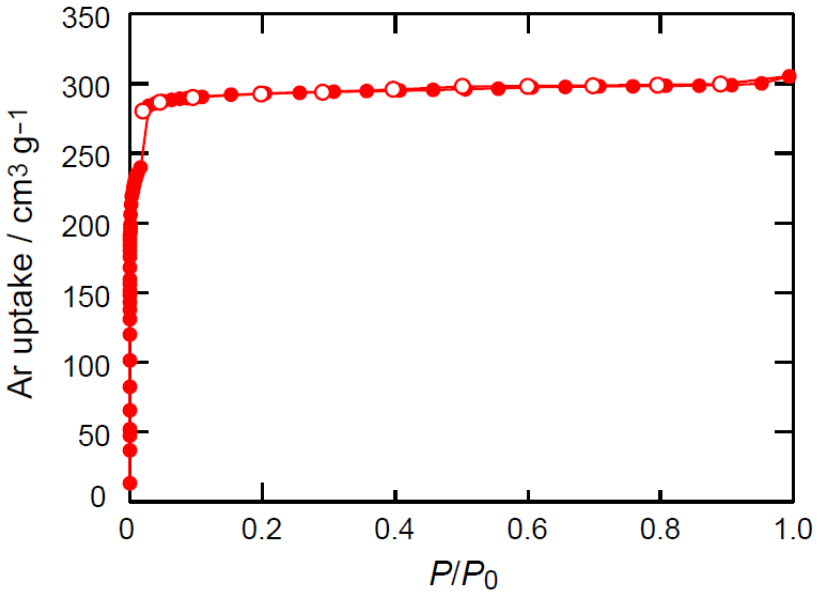

Fig. S16. Ar isotherm at 87 K for activated MOF-646. Filled and open circles represent adsorption and desorption branches, respectively. Connecting traces are guides for the eyes.

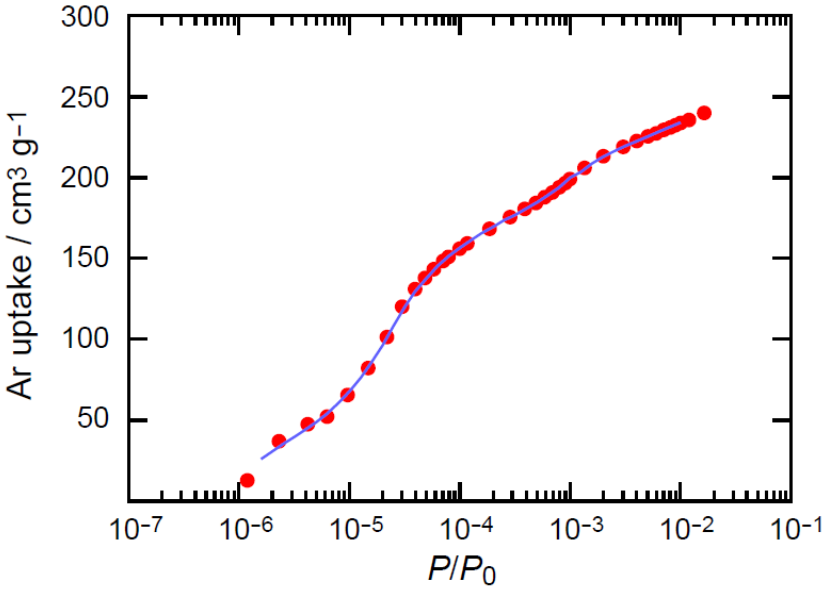

Fig. S17. Ar sorption isotherm at 87 K for activated MOF-646, comparison between experimental (red squares) and NLDFT isotherm (blue solid line).

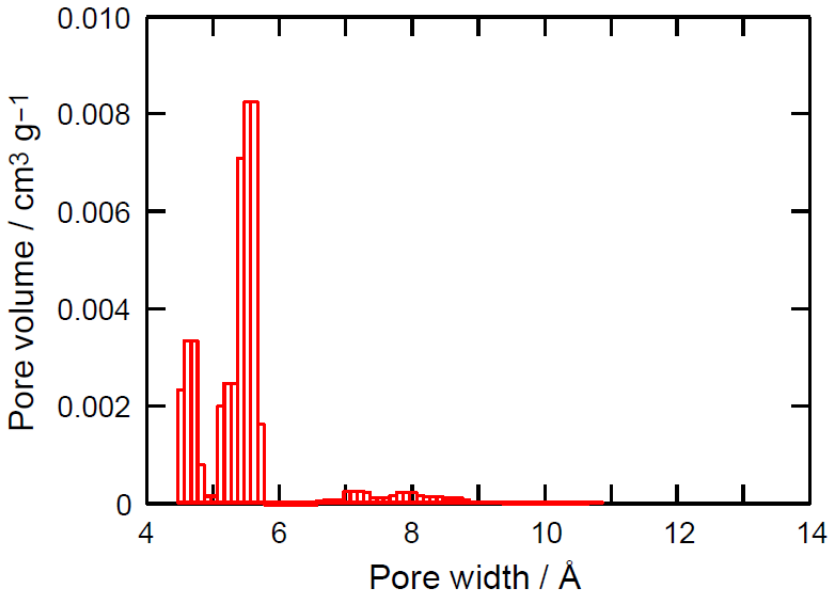

Fig. S18. Pore size distribution (histogram) for activated MOF-646, calculated from a NLDFT fit to the Ar adsorption data for activated MOF-646 in Fig. S17.

Table S2 Summary of N_2 and Ar adsorption measurements for activated MOF-646.

Guest	T / K	Gas uptake / mg g^{-1} [a]	Gas uptake / g L^{-1} [b]	Langmuir SA / m^2 g^{-1}	BET SA / m^2 g^{-1}	Calcd SA / m^2 g^{-1} [c]	PSD / Å [d]	V_p / cm^3 g^{-1}
N_2	77	366	436	1250	1060	1260	N.D.	0.45
Ar	87	545	649	1130	930	1260	4.5/5.5	0.38

[a]Amount of gas adsorbed at P/P_0 = 0.95 of gas pressure. [b]The values are calculated by multiplying the mass of adsorbed gas per gram by the density of the activated MOF-646 (1.19 g cm^{-3}), assuming that the cell volume of MOF-646 is retained in activated MOF-646. [c]The apparent surface area was estimated by using the Langmuir model on activated MOF-646. [d]The pore size distribution (PSD) was calculated from a NLDFT fit to the Ar adsorption data for activated MOF-646 as shown in Fig. S16. [e]The micropore volumes (V_p) were determined using the Dubinin-Raduskavich (DR) transformed N_2 and Ar isotherms across the linear region of the low pressure data.

Estimation of Isosteric Heat of H_2 Adsorption. The isosteric heat of H_2 adsorption was estimated for activated MOF-646 from the H_2 sorption data measured at 77 K and 87 K. A virial-type expression was used (eq 1), which is composed of parameters a_i and b_i that are independent of temperature.[S11] In eq 1, P is the pressure (torr), N is the amount of adsorbed H_2 gas (mg g^{-1}), T is the temperature (K), and m and n represent the number of coefficients required to adequately describe the isotherms.

$$\ln P = \ln N + \frac{1}{T}\sum_{i=0}^{m} a_i N^i + \sum_{i=0}^{n} b_i N^i \qquad (1)$$

To estimate the values of the isosteric heat of H_2 adsorption, eq 2 was applied, where R is the universal gas constant. The isotherms and fitted virial parameters are presented in Fig. S18.

$$Q_{st} = -R\sum_{i=0}^{m} a_i N^i \qquad (2)$$

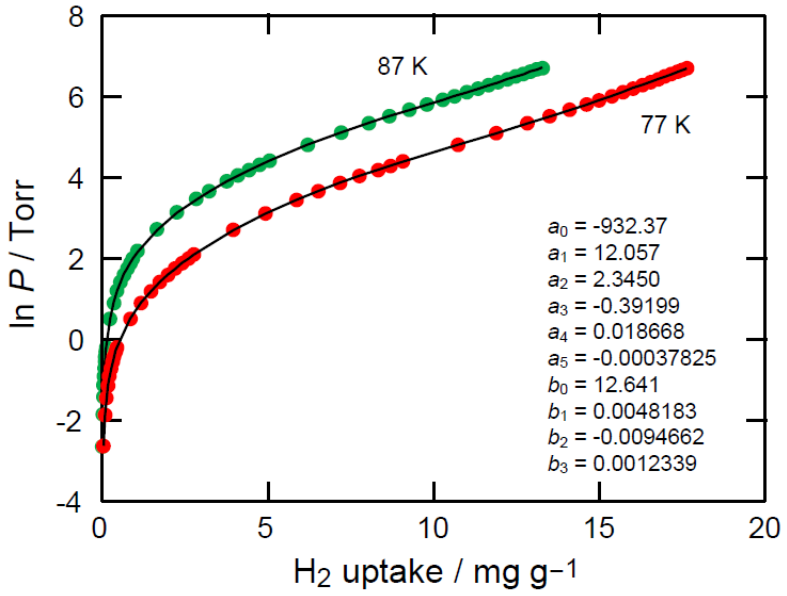

Fig. S19. H_2 isotherms for activated MOF-646 measured at 77 (red) and 87 K (olive). Fitted curves (black solid lines), obtained from the virial-type expansion, were used for the Q_{st} estimation.

Section S8 *References*

[S1] L. J. Mathias and C. G. Overberger, *J. Org. Chem.*, 1980, **45**, 1701.

[S2] Oxford Diffraction (2007). Xcalibur CCD system. Oxford Diffraction Ltd, Abingdon, Oxfordshire, England.

[S3] R. C. Clark and J. S. Reid, *Acta Cryst.*, 1995, **A51**, 887.

[S4] *CrysAlisPro* (Version 1.171.32.41), Oxford Diffraction Ltd, Abingdon, Oxfordshire, England.

[S5] G. M. Sheldrick, *Acta Cryst.*, 2008, **A64**, 112.

[S6] L. J. Farrugia, *J. Appl. Cryst.*, 1999, **32**, 837.

[S7] A. L. Spek, *J. Appl. Cryst.*, 2003, **36**, 7.

[S8] H. Furukawa, M. A. Miller and O. M. Yaghi, *J. Mater. Chem.*, 2007, **17**, 3197.

[S9] J. H. Dymond and E. B. Smith, *The Virial Coefficients of Pure Gases and Mixtures*; Clarendon Press: Oxford, 1980.

[S10] P. I. Ravikovitch, D. Wei, W. T. Chueh, G. L. Haller and A. V. Neimark, *J. Phys. Chem. B*, 1997, **101**, 3671.

[S11] (*a*) J. L. R. Rowsell and O. M. Yaghi, *J. Am. Chem. Soc*., 2006, **128**, 1304; (*b*) M. Dincă, A. Dailly, Y. Liu, C. M. Brown, D. A. Neumann and J. R. Long, *J. Am. Chem. Soc*., 2006, **128**, 16876; (*c*) L. Czepirski and J. Jagiello, *Chem. Eng. Sci.*, 1989, **44**, 797.